

Study of scattered photons from the collimator system of Leksell Gamma Knife using the EGS4 Monte Carlo Code

Joel Y. C. Cheung

Gamma Knife Centre, Canossa Hospital, 1 Old Peak Road, Hong Kong

K. N. Yu^{a)}

Department of Physics and Materials Science, City University of Hong Kong, Tat Chee Avenue, Kowloon Tong, Hong Kong

(Received 17 June 2005; revised 4 November 2005; accepted for publication 7 November 2005; published 19 December 2005)

In the algorithm of Leksell GAMMAPLAN (the treatment planning software of Leksell Gamma Knife), scattered photons from the collimator system are presumed to have negligible effects on the Gamma Knife dosimetry. In this study, we used the EGS4 Monte Carlo (MC) technique to study the scattered photons coming out of the single beam channel of Leksell Gamma Knife. The PRESTA (Parameter Reduced Electron-Step Transport Algorithm) version of the EGS4 (Electron Gamma Shower version 4) MC computer code was employed. We simulated the single beam channel of Leksell Gamma Knife with the full geometry. Primary photons were sampled from within the ^{60}Co source and radiated isotropically in a solid angle of 4π . The percentages of scattered photons within all photons reaching the phantom space using different collimators were calculated with an average value of 15%. However, this significant amount of scattered photons contributes negligible effects to single beam dose profiles for different collimators. Output spectra were calculated for the four different collimators. To increase the efficiency of simulation by decreasing the semiaperture angle of the beam channel or the solid angle of the initial directions of primary photons will underestimate the scattered component of the photon fluence. The generated backscattered photons from within the ^{60}Co source and the beam channel also contribute to the output spectra. © 2006 American Association of Physicists in Medicine. [DOI: 10.1118/1.2143138]

Key words: scattered photons, Monte Carlo, Leksell Gamma Knife

I. INTRODUCTION

The Leksell Gamma Knife contains ^{60}Co as radiation source, with the output spectrum consisting of two photon peaks at 1.17 and 1.33 MeV. Scattered photons will be generated mainly due to the Compton effect when primary photons interact with the cobalt pellets, the source capsule, and the collimator system. In the algorithm of Leksell GAMMAPLAN, these scattered photons are presumed to have negligible effects in Gamma Knife dosimetry. In this study, we used the EGS4 Monte Carlo (MC) technique to study the scattered photons coming out of a single beam channel of Leksell Gamma Knife. Primary photons were sampled from within the ^{60}Co source and radiated isotropically in a solid angle of 4π .

The Monte Carlo technique has been widely employed in the field of Gamma Knife radiosurgery and accurate results have been obtained for many difficult physical situations.¹⁻⁸ Similar calculations concerning scattered photons have been performed previously.^{7,8} In these studies, however, the output spectra were different significantly with orders of magnitude difference between the unscattered and scattered photon peaks. The low energy backscattered photons from within the source and the beam channel were ignored. The initial directions of the quanta have been sampled in a cone with a certain degree of semiaperture in order to increase the efficiency of simulation and therefore no backscattered photons can be

created. These backscattered photons, however, contribute to the output spectra and will be underestimated in the scattered component of output photon spectra. This is an interesting issue and will be studied in the present paper.

II. MATERIALS AND METHODS

The PRESTA (Parameter Reduced Electron-Step Transport Algorithm) version^{9,10} of the EGS4 (Electron Gamma Shower version 4) MC computer code was employed. Detailed descriptions of the structure of the EGS4 code can be found in the reference by Nelson *et al.*¹¹ In order to study the scattered photons, we simulated the Gamma Knife single beam channel with the full geometrical description.^{7,8,12,13} The sealed source is composed of 20 ^{60}Co pellets, each of them 1 mm in diameter and 1 mm in length. The sources are doubly encapsulated in 300 series stainless steel (C 0.1%, Si 0.7%, Cr 18.0%, Mn 1.0%, Fe 71.2%, Ni 9.0%) with welded closures. The nominal dimensions of the source capsule are 0.31 in. (7.9 mm) in diameter and 1.07 in. (27.2 mm) long, including cobalt pellets, inner and outer containers. Each beam channel consists of a precollimator of 65-mm-thick tungsten alloy (Ni 3.5%, Cu 1.5%, W 95.0%) and a 92.5-mm-thick lead collimator. The interchangeable final collimator is made of 60-mm-thick tungsten alloy. The available sizes of the interchangeable final collimator are 4, 8, 14, and 18 mm. Primary photons are sampled from within the source

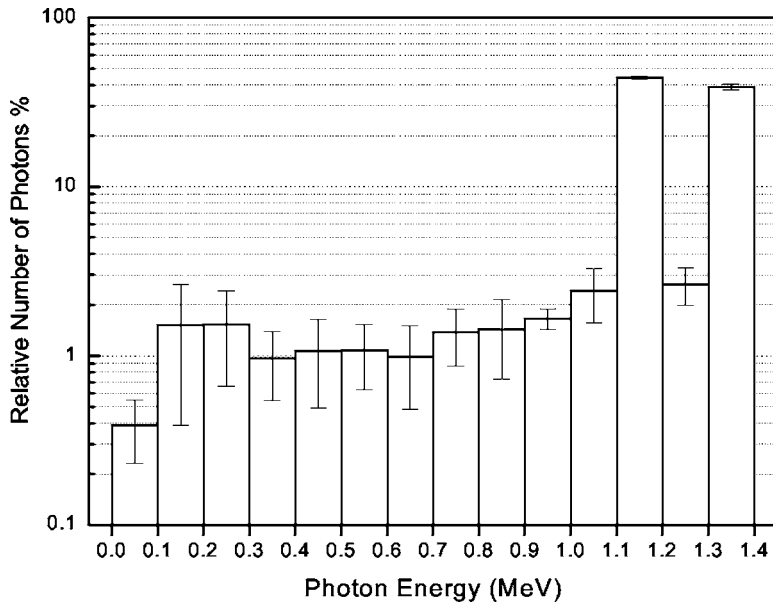


FIG. 1. Monte Carlo results of an output spectrum for the 4 mm collimator system. The error bars represent one standard deviation.

isotropically in a 4π solid angle. Scattered photons will be generated through Compton scattering within the source and the single beam channel. The Rayleigh scattering (coherent scattering) only broadens the angular width of a beam slightly.

The patient's head or spherical water phantom is assumed to be absent. Exiting photons reaching the phantom space (a sphere of 160 mm diameter centered at the unit center point) were scored. The unit center point has a coordinate $x=100$, $y=100$, and $z=100$ with a distance of 400 mm from any ^{60}Co source. History runs of 1.5×10^8 , 6.5×10^7 , 4.5×10^7 , and 3×10^7 were performed for the 4, 8, 14, and 18 mm collimators, respectively. On average, the simulation time for a history run of 10^4 took 202 s on a Pentium II 550 PC with installed POWERSTATION 4.0 FORTRAN compiler and WINDOWS 98. As mentioned earlier, the photon spectrum of ^{60}Co

has two peaks, viz. 1.173 and 1.333 MeV. It was assumed that the emitted beta electrons do not come out of the source capsules, therefore there were no simulations using the beta spectrum from ^{60}Co decay. The cut-off energies for electrons and photons were set to be 0.521 and 0.01 MeV, respectively. Lowering the value of these cut-off energies showed no significant differences in the dose distribution. The latest collision and radiative stopping powers of ICRU 37¹⁴⁻¹⁶ were employed in the PEGS4 (pre-processor of EGS4) data file.¹⁷ Since all simulations required huge numbers of history runs, a long sequence random number generator from James¹⁸ was used. This random number generator possesses a sequence length of about 10^{43} , effectively infinite for our calculations, and has about 10^9 independent sequences that can be selected from initial conditions. Rayleigh scattering, photoelectron angle selection,¹⁹ and bremsstrahlung angle

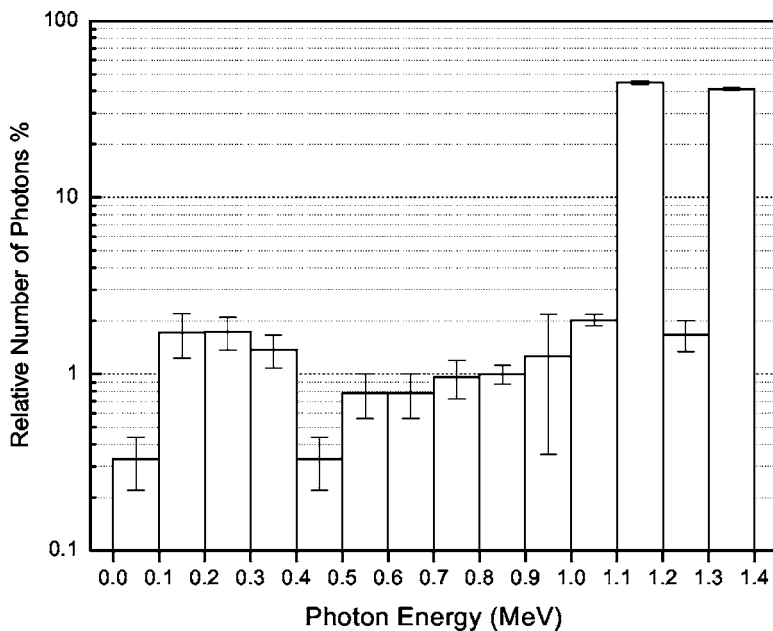


FIG. 2. Monte Carlo results of an output spectrum for the 8 mm collimator system. The error bars represent one standard deviation.

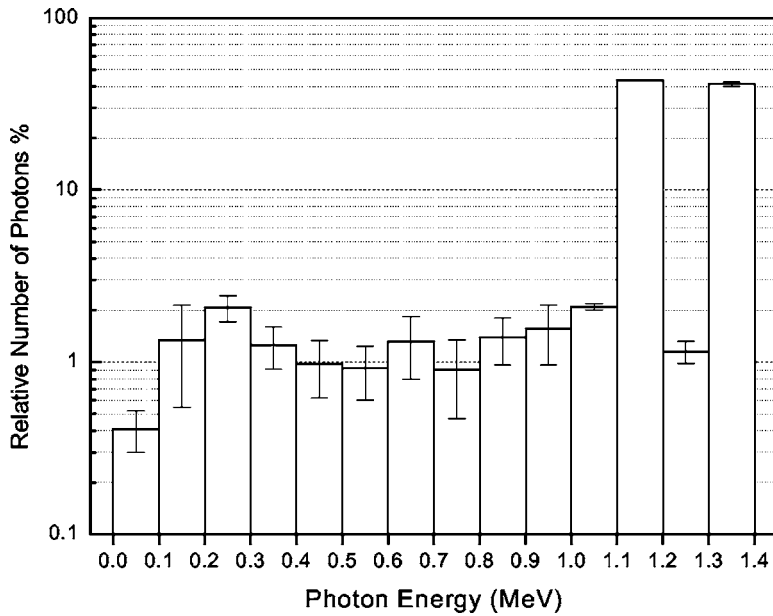


FIG. 3. Monte Carlo results of an output spectrum for the 14 mm collimator system. The error bars represent one standard deviation.

selection²⁰ were turned on in all calculations.

III. RESULTS AND DISCUSSION

Figures 1–4 show the MC results of the output spectra for the 4, 8, 14, and 18 mm single beam channels with the full geometry. The overall profiles of these spectra are similar and the difference between the number of scattered and unscattered photons has a similar order of magnitude as the measured spectra of Mack *et al.*²¹ Table I shows the percentage yields of scattered photons (i.e., the ratio between the number of scattered photons and the total number of photons) for different collimators. The percentage yields are similar for different collimators with an average value of 15%. A few secondary electrons can only be scored for all collimators in runs with a history number on the order of 10^7 .

The Compton effect (incoherent scattering) is the dominant photon interaction process within the collimator system. The probability of a recoil electron going almost in the forward direction is extremely small.²² Further increase in the number of histories in order to obtain a better statistics for scoring the secondary electrons is difficult, since it requires a very long simulation time.

Similar calculations have been performed previously.^{7,8} In these works, the low energy backscattered photons from the source and the beam channel have been ignored. These generated backscattered photons however contribute to the output spectra. The initial directions of the quanta have been sampled in a cone with a 3° or 10° of semiaperture in order to increase the efficiency of simulation. The statistics of both exiting photons and secondary electrons can then be im-

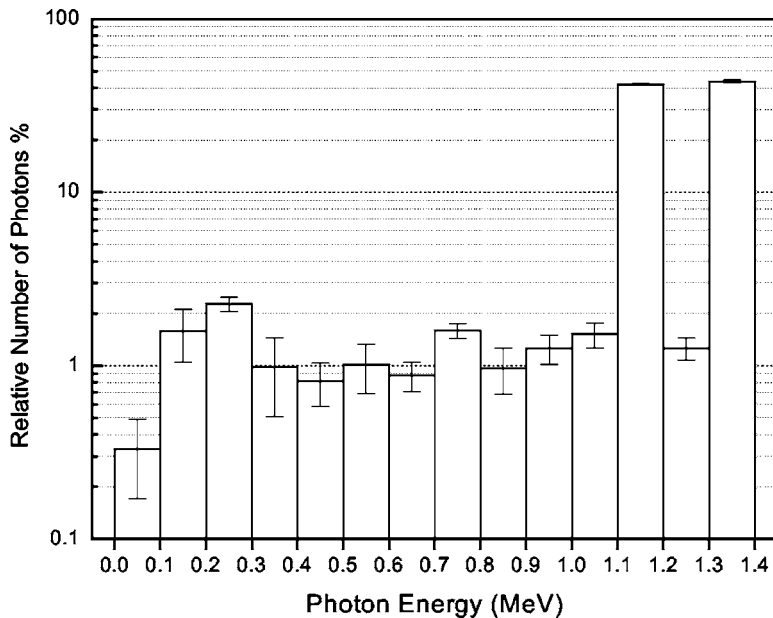


FIG. 4. Monte Carlo results of an output spectrum for the 18 mm collimator system. The error bars represent one standard deviation.

TABLE I. Percentage yields of scattered photons for different collimators.

Collimator system (mm)	Percentage yield of scattered photons
4	17.1 ± 1.4
8	14.0 ± 0.8
14	15.4 ± 0.9
18	14.5 ± 0.8

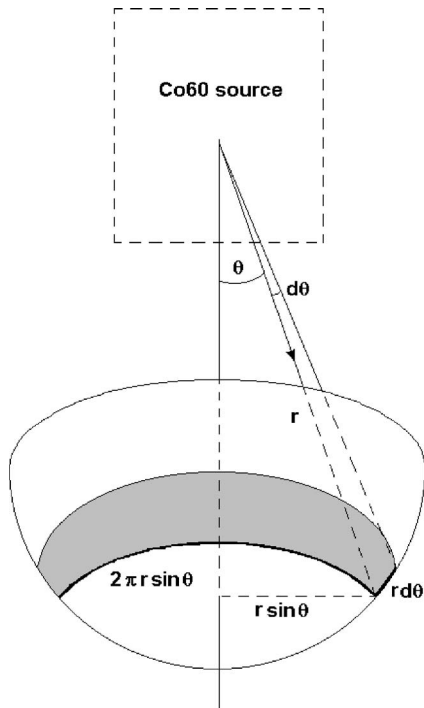


FIG. 5. The conversion between semiapertures θ and solid angles Ω . The solid angles Ω subtended by the angle θ are equal to the surface area subtended by the angle θ divided by r^2 , since one solid angle steradian has an area of r^2 .

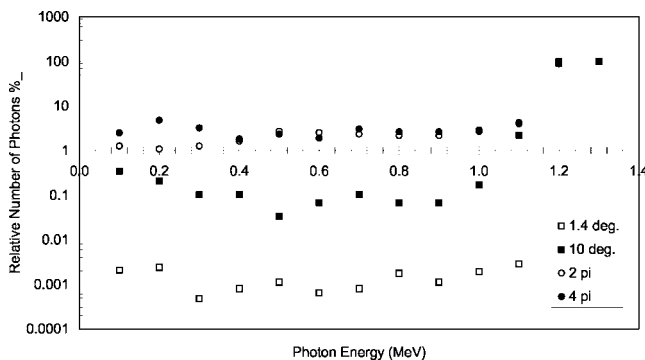


FIG. 6. Comparison of output spectra for the 18 mm collimator system using different semiapertures and steradian solid angles. The uncertainties of the relative number of photons were less than 9%.

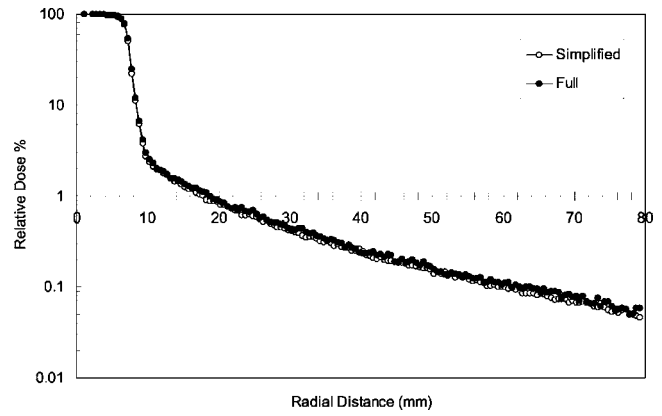


FIG. 7. Comparison of single beam dose profiles simulated in water for the 14 mm collimator with full and simplified geometry.

proved dramatically. To see the difference, we repeated our simulations using different semiapertures and solid angles for the initial directions of the quanta. For easy comparison, the conversion between semiapertures θ and solid angles Ω is given by

$$\Omega = \frac{1}{r^2} \int_0^\theta 2 \cdot \pi \cdot r \cdot \sin \theta \cdot r d\theta$$

(see Fig. 5), i.e., $\theta=90^\circ$ corresponds to $\Omega=2\pi$. Figure 6 shows the comparison among the output spectra for the 18 mm collimator system using different semiapertures (1.4° and 10°) and solid angles (2π and 4π). The use of small semiapertures will underestimate the scattered component of the photon fluence. The use of a solid angle of 2π gives comparable results to those for a solid angle of 4π . This is because the use of a 2π solid angle will ignore fewer back-scattered photons when compared to the cases using the semiapertures of 1.4° and 10° .

Single beam dose profiles in a water equivalent phantom (8 cm depth at the unit center point of the phantom) were generated by the full geometry model and a simplified model for different collimators, from which we found no observable differences (see Fig. 7). Furthermore, we found no signifi-

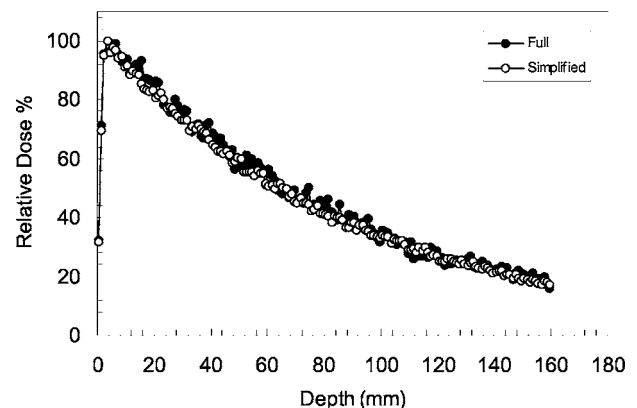


FIG. 8. Comparison of depth dose curves simulated in water for a single beam using 14 mm collimator with full and simplified geometry.

TABLE II. Internal diameters for different final exchangeable collimators.

Collimators (mm)	4	8	14	18
Incoming diameter	2.14	3.92	6.52	8.26
Exiting diameter	2.66	5.00	8.56	10.88

cant differences between the depth dose curves (Fig. 8) simulated in the water equivalent phantom of a single beam using the 14 mm collimator with full and simplified geometry models. For the simplified model, each source was modeled by a cylinder 1 mm in diameter and 20 mm in length without the source and capsule filtration. The source center was positioned at a distance of 400 mm from the center of the phantom. The diameters of radiation beams at the focus were confined mathematically by the internal diameters of the interchangeable final collimators (see Table II). The directions of primary photons were sampled only if the photons were able to pass through the internal diameters. In this model, no scattered photons can be generated. The obtained 15% of scattered photons, however, do not affect the overall single-beam dose profiles. The reason is that the scattered photons as well as the unscattered primary photons will be scattered and create secondary electrons and lose energy during interactions with the water phantom. A large amount of multiple scattered photons in the water phantom created by the unscattered photons will “wash out” the effects of 15% scattered photons. The influence upon the dose distribution of bremsstrahlung generated by the secondary electrons in water can be neglected. On average, one primary photon with energy of 1.333 or 1.173 MeV will create 0.88 ± 0.03 bremsstrahlung photons with a mean energy of 8.22 keV and a standard deviation of 10.13 keV during the interactions with the phantom. Furthermore, some of the low-energy scattered photons are stopped at the superficial part of the phantom. The use of the simplified model can improve the efficiency in Gamma Knife MC simulations and is able to save the computer time by an average factor of 5.7.

IV. CONCLUSIONS

The overall shapes of the output photon spectra are similar for different collimators sizes. The percentage yield of scattered photons was calculated with an average value of 15%. However, this significant amount of scattered photons does not affect the overall single beam dose profiles when considering the cases with and without the scattered photons.

We suggest that primary photons should be sampled from those within the ^{60}Co sources and radiate isotropically in a 4π solid angle in order to calculate the accurate output spectra of the Leksell Gamma Knife. On the other hand, the solid angle can be reasonably reduced only when calculating dose profiles in phantoms.

^{a)}Electronic mail: peter.yu@cityu.edu.hk

¹V. Moskvina, R. Timmerman, C. DesRosiers, M. Randall, P. DesRosiers, P.

Dittmer, and L. Papiez, “Monte Carlo simulation of the Leksell Gamma Knife. II. Effects of heterogeneous versus homogeneous media for stereotactic radiosurgery,” *Phys. Med. Biol.* **49**, 4879–4895 (2004).

²F. M. Al-Dweri and A. M. Lallena, “A simplified model of the source channel of the Leksell Gamma Knife: Testing multisource configurations with PENELOPE,” *Phys. Med. Biol.* **49**, 3441–3453 (2004).

³J. Y. C. Cheung, K. N. Yu, C. P. Yu, and T. K. Ho, “Monte Carlo calculation of single-beam dose profiles used in a gamma knife treatment planning system,” *Med. Phys.* **25**, 1673–1675 (1998).

⁴J. Y. C. Cheung, K. N. Yu, C. P. Yu, and T. K. Ho, “Monte Carlo calculated output factors of a Leksell Gamma Knife unit,” *Phys. Med. Biol.* **44**, N247–N249 (1999).

⁵Y. C. Cheung, K. N. Yu, C. P. Yu, and T. K. Ho, “Stereotactic dose planning system used in Leksell Gamma Knife model-B: EGS4 Monte Carlo versus GafChromic films MD-55,” *Appl. Radiat. Isot.* **53**, 427–430 (2000).

⁶J. Y. C. Cheung, K. N. Yu, C. P. Yu, and T. K. Ho, “Dose distributions at extreme irradiation depths of gamma knife radiosurgery: EGS4 Monte Carlo calculations,” *Appl. Radiat. Isot.* **54**, 461–465 (2001).

⁷V. Moskvina, C. DesRosiers, L. Papiez, R. Timmerman, M. Randall, and P. DesRosiers, “Monte Carlo simulation of the Leksell Gamma Knife. I. Source modelling and calculations in homogeneous media,” *Phys. Med. Biol.* **47**, 1995–2011 (2002).

⁸F. M. O. Al-Dweri, A. M. Lallena, and M. Vilches, “A simplified model of the source channel of the Leksell GammaKnife® tested with PENELOPE,” *Phys. Med. Biol.* **49**, 2687–2703 (2004).

⁹A. F. Bielajew and D. W. O. Rogers, “Electron Step-size Artefacts and PRESTA,” in *Monte Carlo Transport of Electrons and Photons*, edited by T. M. Jenkins, W. R. Nelson, and A. Rindi (Plenum, New York, 1988), p. 115.

¹⁰A. F. Bielajew and D. W. O. Rogers, “PRESTA: The Parameter Reduced Electron-Step Transport Algorithm for Electron Monte Carlo Transport,” NRC-CNRC, 1988.

¹¹W. R. Nelson, H. Hirayama, and D. W. O. Rogers, “The EGS4 Code System SLAC-265,” Stanford Linear Accelerator Center, Stanford University, Stanford, CA 94305 (<http://www.slac.stanford.edu/egs/>), 1985.

¹²Y. C. Cheung, K. N. Yu, C. P. Yu, and T. K. Ho, “Quality assurance of stereotactic treatment planning system: Implementation of Monte Carlo technique on Leksell Gamma Knife,” *Proceedings of the Sixth International Conference on Medical Physics*, Patras, Greece, 1–4 September 1999, Monduzzi Editore (International Proceedings Division) S.p.A.–Bologna, Italy, pp. 95–99.

¹³Elekta Instrument–Stockholm, Registry of Radioactive Sealed Sources and Devices (Safety Evaluation of Sealed Source), 1984.

¹⁴ICRU, “Stopping powers for electrons and positrons,” ICRU Report No. 37 (USGPO, Washington, DC, 1984).

¹⁵S. Duane, A. F. Bielajew, and D. W. O. Rogers, “Use of ICRU-37/nbs collision stopping power in the EGS4 system,” National Research Council of Canada Report No. PIRS-0173, 1989.

¹⁶D. W. O. Rogers, S. Duane, and A. F. Bielajew, “Use of ICRU-37/nbs radiative stopping power in the EGS4 system,” National Research Council of Canada Report No. PIRS-0177, 1989.

¹⁷W. R. Nelson, “Lecture-9 on PEGS4: Datasets for different media,” in course on electron and photon transport using the EGS4 Monte Carlo system 25–28 September 1989, National Physical Laboratory, Teddington, UK, 1989.

¹⁸F. James, “A review of pseudorandom number generators,” CERN-DATE handling division, Report No. dd/88/22, 1988.

¹⁹A. F. Bielajew and D. W. O. Rogers, “Photoelectron angular distribution in the EGS4 code system,” National Research Council Canada PIRS-0058, 1986.

²⁰A. F. Bielajew, R. Mohan, and C. S. Chui, “Improved bremsstrahlung photon angular sampling in the EGS4 code system,” National Research Council of Canada Report No. PIRS-0203, 1989.

²¹A. Mack, S. G. Scheib, J. Major, S. Gianolini, G. Pazmandi, H. Feist, H. Czempel, and H. J. Kreiner, “Precision dosimetry for narrow photon beams used in radiosurgery—Determination of Gamma Knife(R) output factors,” *Med. Phys.* **29**, 2080–2089 (2002).

²²H. E. Johns and J. R. Cunningham, *The Physics of Radiology*, 4th ed. (Thomas, Springfield, IL, 1983).